Experimental Thermal and Fluid Science 95 (2018) 81–87

Contents lists available at ScienceDirect

Experimental Thermal and Fluid Science

journal homepage: www.elsevier.com/locate/etfs

# Dynamics of acoustically forced non-premixed flames close to blow-off

Anna-Maria Kypraiou*, Andrea Giusti, Patton M. Allison, Epaminondas Mastorakos

*Department of Engineering, University of Cambridge, Cambridge CB2 1PZ, UK*

ARTICLE INFO

*Keywords:*
Non-premixed flame
Blow-off
Lean blow-off limits
Acoustic oscillations
Thermoacoustics
Lift-off height

ABSTRACT

The effect of forced oscillations on the behaviour of non-premixed swirling methane flames close to the lean blow out limits was investigated using experiments in a lab-scale burner. Two different fuel injection geometries, non-premixed with radial -NPR- and non-premixed with axial -NPA- fuel injection, are considered. The flame behaviour is studied using 5 kHz OH* chemiluminescence and OH Planar Laser Induced Fluorescence (OH PLIF) imaging. In both systems, acoustic forcing reduces the stability of the flame, and in particular, the stability was found to decrease with the increase in forcing amplitude. Flame lift-off was observed in both configurations, with the magnitude of the effect of forcing depending on the fuel injection configuration. The results provide insight on the effect of superimposed flow field fluctuations in systems operating close to the lean blow out limits and offer useful data for the development and validation of numerical models for the prediction of the dynamic behaviour of flames of industrial interest.

## 1. Introduction

In order to reduce the environmental impact of combustion systems, and in particular to reduce $NO_x$ emissions, gas turbine manufacturers are developing technologies based on the use of lean flames. However, lean combustion systems are more prone to combustion instabilities [1], which are becoming one of the main issues for the development of lean burn technologies. Combustion instabilities can cause vibration and additional noise [2], and in the case of large fluctuations, also flame quenching, flashback and damages of the combustor components [3].

The study of the flame behaviour in the presence of flow field fluctuations is very important for the understanding of combustion instabilities and in general for the development of modern combustors based on lean burn technology. Self-excited oscillations can affect the local behaviour of the flame [4–6], possibly involving local extinction and re-ignition phenomena. Furthermore, as observed in Refs. [7–9], the presence of velocity oscillations can have a strong impact on the stability limits (in the sense of flame existence, not in the sense of absence of pressure oscillations) of the flame. The understanding and prediction of flame blow-off is of crucial importance for the design of modern combustors that often operate close to the lean blow out limits. Therefore, it is also of great interest to study the impact of periodic motions on the local and global extinction of flames of practical interest.

Several fundamental studies on the effect of velocity fluctuations on the local flame behaviour can be found in the literature. Among them, Sung and Law [4] investigated the transient behaviour of counterflow diffusion and premixed flames subjected to sinusoidal velocity fluctuations. The flame structure of the premixed flame was found to be less sensitive to the fluctuations of the strain rate compared to diffusion flames. Furthermore, the amplitude of the flame response was found to decrease with the increase in the frequency of the oscillations. As far as extinction is concerned, the same study showed that for low forcing frequencies the extinction strain rate is independent of mean strain rate [4] (the variations of the strain rate are sufficiently slow compared to the chemical time scale and the flame responds to the local value of the strain). In contrast, for high frequencies, the extinction behaviour depends on the amplitude of the fluctuations and the effective Lewis number of the mixture [4]. A similar behaviour was also found in [5,6], where the effect of oscillations of the strain rate on diluted methane counterflow diffusion flames was investigated. Both studies showed that at high frequencies the peak strain rate can be extended further beyond the steady-state extinction limit. Furthermore, the amplitude of the strain that a flame can sustain without extinguishing depends on the value of the mean strain rate and generally decreases with the increase in the mean strain [5].

Considering flame configurations much closer to real engines, limited literature exists on the investigation of the effect of acoustic oscillations in conditions close to the lean blow out limits. Furthermore, the focus is usually on premixed flames only [7,8,10]. In one of these studies [8] the blow-off of bluff-body stabilised premixed flames under harmonic forcing of the upstream mixture velocity was investigated. The results suggest that the presence of velocity fluctuations has a strong impact on the flame behaviour, and both the blow-off mechanism and stability limits of forced flames can be different from the one observed in unforced flames. These investigations have been

* Corresponding author.
*E-mail address:* amk74@cam.ac.uk (A.-M. Kypraiou).

https://doi.org/10.1016/j.expthermflusci.2018.01.036
Received 28 January 2018; Accepted 29 January 2018
Available online 31 January 2018

further extended to include upstream spatial mixture gradients [9,11]. Results show that the behaviour of the flame and the blow-off limits are strongly affected by the spatial variation of the equivalence ratio upstream of the reacting region. Since many practical systems operate in conditions where fuel and air are not fully premixed before entering the combustion zone, it is of great interest to further extend the study of the response of flames with spatial variation of the equivalence ratio to configurations much closer to practical devices. In the case of imperfect premixing, the time-varying velocity field may introduce time-varying and spatially-varying equivalence ratio distributions, or in the case of fully non-premixed systems, time-varying heat release rate due to the time-varying mixing rates. Hence, the study of the forced response of systems characterised by different levels of premixing could also allow us to explore the impact of different mechanisms on the flame stability.

In this work, the effect of air fluctuations on the behaviour of swirling flames at conditions close to the lean blow out limits has been investigated using experiments. Two configurations, characterised by different fuel injection strategies, have been considered to include spatial variations of the equivalence ratio up to fully non-premixed systems. The present investigation extends forced flame studies towards the case of flames close to their overall stability limits and, at the same time, extends the typical lean blow out studies to the case of forced air fluctuations. The specific objectives are: (i) to understand the effect of forcing amplitude on the flame characteristics and lean blow out limits in systems characterised by different fuel injection; (ii) to give more insight into the flame structure and the mechanisms affecting local and global extinction; (iii) to measure the effect of forced fluctuations on the lift-off height of stable flames at conditions far and close to blow-off.

## 2. Materials and methods

The experimental apparatus used in this study is a modified version of the rig used in previous blow-off studies without forcing [12,13]. The main differences are the presence of a system upstream of the flame region to create the forced fluctuations and the fuel injection configuration (a geometry with radial fuel injection has been added). Two fuel configurations were studied in this work: (a) non-premixed methane flames with radial fuel injection (NPR) and (b) non-premixed flame with and axial fuel injection (NPA). A schematic of the experimental rig is shown in Fig. 1. The burner consisted of two long concentric circular ducts. The outer duct (i.d. = 37 mm) housed two pressure taps (axial distance = 200 mm), where pressure transducers were mounted flush with the duct internal wall for acoustic pressure measurements. At the exit of the inner duct (i.d. = 6 mm), a conical bluff body of diameter 25 mm was mounted. A 60-degree vane angle swirler, located 41.6 mm upstream of the bluff body plane, created an azimuthal component of the velocity at the exit. For inert conditions, the velocity measurements of Ref. [14] showed that the tangential velocity was about 0.5 $U_b$, where $U_b$ is the bulk axial velocity. This measurement was taken at the centre of the annular passage, between the bluff body and the outer duct, and at an axial distance of 6 mm downstream of the bluff body plane. Inside the plenum flow straighteners streamlined the flow. Four quartz plates of 97 mm width and 150 mm length enclosed the working section and provided optical access to the flame, preventing any possible air entrainment from the surroundings. In order to perturb the flame and thus induce heat release fluctuations, acoustic oscillations were imposed to the air mass flow by means of two loudspeakers, positioned diametrically opposite each other in a plenum, which was fitted upstream of the outer duct. The flames were forced at 160 Hz (main resonant frequency of the plenum and burner assembly [15], chosen on purpose in order to achieve a high forcing amplitude), while the forcing amplitude varied to investigate its effect on the blow-off dynamics. The main difference between the NPR and NPA systems is the fuel injection point. In the bluff body of the NPR system the fuel was injected radially through a 0.5 ± 0.01 mm circular gap located 3 mm upstream of the bluff body plane (Fig. 1). In this system, apart from the time-varying velocity field, there was also a time- (the fuel flow could in principle oscillate, since the annular gap at the injection point was not choked) and space-varying equivalence ratio. In the NPA system, the bluff body design was modified so that a central pipe of diameter of 4 mm fed the methane, as shown in Fig. 1. Air and fuel flow rates were controlled using Alicat mass flow controllers.

The operating conditions are presented in Table 1 together with the acronyms that will be used in the remainder of this paper to indicate each condition. The air velocity was calculated as the air flow rate divided by the open annular area between the bluff-body and the outer duct at the exit of the burner inlet, while the fuel velocity was calculated as the fuel flow rate divided by the area of the fuel nozzle exit. The flame behaviour for every case was characterised by means of: (i) velocity fluctuations at the bluff-body edge (indirect measurement through the two-microphone technique), (ii) $OH^*$ chemiluminescence,

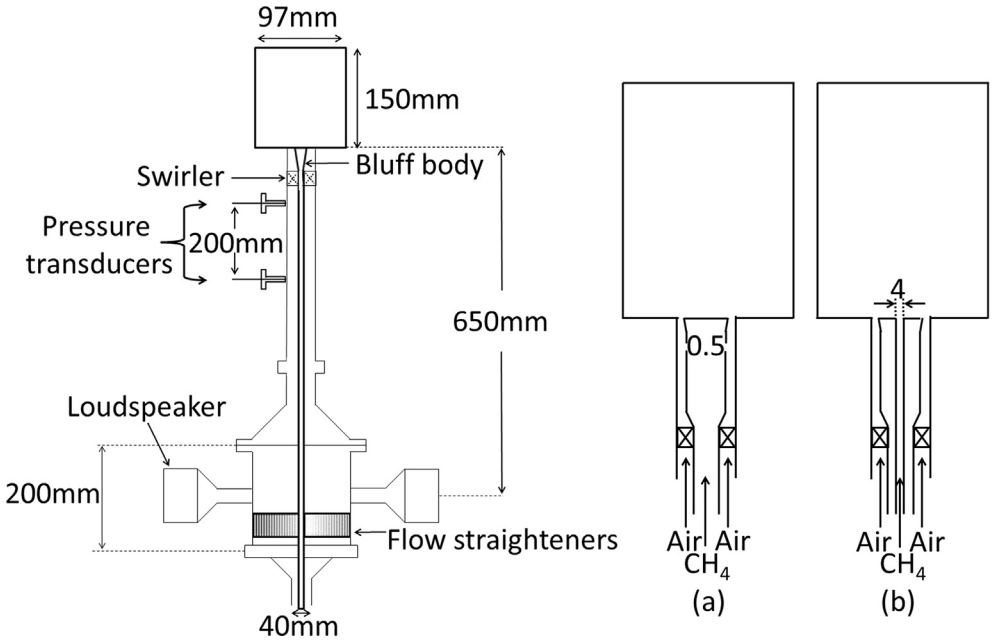


**Fig. 1.** Schematic of the burner used for the blow-off study of forced (a) NPR and (b) NPA flames.

**Table 1**
Experimental conditions of non-premixed flames with radial (NPR) and non-premixed flames with axial (NPA) fuel injection.

| Condition | $U_{air}$ (m/s) | $U_{fuel}$ (m/s) | Global φ | Air flow rate (lpm) | Methane flow rate (lpm) |
|---|---|---|---|---|---|
| *Blow-off visualisation* | | | | | |
| NPR-15-050 | 15 | 36.3 | 0.50 | 530 | 27.4 |
| NPA-15-030 | 15 | 22.3 | 0.30 | 530 | 16.8 |
| *Lift-off height statistics* | | | | | |
| NPR-15-055 | 15 | 16.5 | 0.55 | 530 | 30 |
| NPR-15-070 | 15 | 21.4 | 0.70 | 530 | 39 |
| NPA-15-038 | 15 | 28.5 | 0.38 | 530 | 21.5 |
| NPA-15-042 | 15 | 31.8 | 0.42 | 530 | 24 |

(iii) OH PLIF. These will be described next, together with the experimental procedure used to evaluate the blow-off under forced conditions and the statistics of the flame lift-off.

Two Kulite pressure transducers (Model XCQ-093) were used to measure pressure oscillations. Time series of acoustic pressure were analysed spectrally using the Fast Fourier Transform (FFT) technique in order to determine the complex amplitude of $u'$ at the forcing frequency by means of the two-microphone technique [16]. The peak value of the fluctuation was then normalised using the respective time averaged value to obtain the non-dimensional forcing amplitude, $A = u'(f)/\langle u \rangle$. The two-microphone technique was checked using direct measurements of velocity fluctuations under cold flow conditions with a Dantec hot wire anemometer (Model 55P11).

The $OH^*$ chemiluminescence measurements were conducted using: (i) full planar view high-speed imaging system, and (ii) a photo-multiplier tube (PMT) unit. In particular, the high-speed imaging system consisted of a LaVision IRO high-speed two stage intensifier (spectral range of 190–800 nm) coupled to a Photron SA1.1 monochrome high-speed CMOS camera with a 1024 × 1024 pixel resolution up to 5.4 kHz. A UV bandpass filter (270–370 nm) was fitted to the Cerco 2178 UV camera lens. Images were recorded at 5 kHz for 1 s within the pressure measurement period and the intensifier gated at 190 μs. The projected pixel resolution was approximately 0.14 mm/pixel. The photo-multiplier tube used to measure the global $OH^*$ chemiluminescence was a Thorlabs PMT (Model PMM01), fitted with the UV bandpass filter (270–370 nm). The PMT measurements were recorded simultaneously with the pressure measurements. Experimental data were recorded with a National Instruments data acquisition system controlled by the Labview software program at a sampling frequency of 10 kHz.

The OH PLIF system consisted of a SIRAH Credo high speed dye laser (Model 2400), pumped by a high-repetition rate diode solid state laser (532 nm, Model JDSU Q201-HD), with a power of 14 W at 5 kHz and a pulse length of around 18 ns. The dye laser produced a beam at 566 nm, which was doubled by a BBO crystal to produce a beam with an average power of 300 mW at 5 kHz (60 μJ/pulse). The laser beam was expanded to a 40 mm-height sheet using optics, and the laser sheet thickness was 0.23 mm. A LaVision IRO high-speed two stage intensifier was used, coupled to the aforementioned high-speed camera, fitted with a UV bandpass filter (300–325 nm). Images were recorded at 5 kHz for 1 s, within the pressure measurement period, and the intensifier gated at 400 ns. The resolution of OH PLIF images was approximately 0.1 mm/pixel. During processing, each instantaneous OH PLIF image was initially filtered using a 2-D median nonlinear filter for noise reduction (3 × 3 filter size). Then, the filtered images were corrected for laser sheet profile inhomogeneities with a Gaussian intensity profile.

In order to determine the blow-off point, for a constant air flow rate and a given forcing amplitude, $A$, the fuel flow rate was decreased gradually in steps of 0.1 lpm every 40 s, until blow-off occurred, recording the fuel blow-off flow rate. At each air flow rate, an average fuel blow-off flow rate of 10 individual measurements was calculated and reported in Fig. 2.

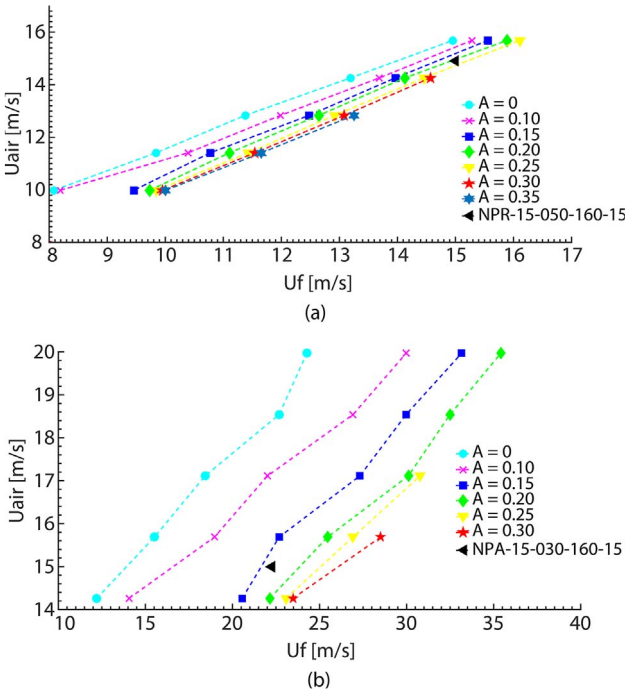


**Fig. 2.** Air blow-off velocity, $U_{air}$, as a function of fuel blow-off velocity, $U_f$, (calculated at the exit of the fuel nozzle), for various forcing amplitudes $A$, for (a) the non-premixed with radial and (b) non-premixed with axial fuel injection configurations.

For the lift-off height estimation, the instantaneous OH PLIF images were filtered with a Gaussian filter of a width of 3 pixels to remove high frequency noise, and then they were converted into binary images using an intensity thresholding algorithm. Binary values were assigned to the progress variable, which was defined such that it took a value of 0 in fresh reactants and a value of 1 in burnt gases. Also, the magnitude of the 2-D gradient of the progress variable was calculated and the instantaneous flame edge contour was obtained using a threshold on the gradient. The distance of the high gradient of OH regions from the bluff body edge of the left and right branch of the flame was estimated for each image and was referred to as lift-off height, $h$. The probability density function (PDF) of the lift-off height was estimated and the power spectral density (PSD) of the lift-off height was obtained. It should be noted that the duration of the OH PLIF imaging was long enough to capture all the temporal scales/features of the flame. Thus, the use of OH PLIF measurements for the estimation of the lift-off height statistics presented in this work is valid. In particular, the flow is axi-symmetric, thus the statistics are axi-symmetric, and a 2-D cut is sufficient for the present application.

## 3. Results

The lean blow out limits of the forced NPR and NPA systems were investigated for various forcing amplitudes in order to study the influence of air flow oscillations on the blow-off behaviour. Then, the blow-off event of forced NPR and NPA flames was studied qualitatively with flame visualisation using $OH^*$ chemiluminescence and OH PLIF imaging, but also quantitively by recording the duration of the blow-off transient. Finally, the probability density function (PDF) of the lift-off height for flames at conditions close and far from blow-off was estimated.

### 3.1. Effect of forcing amplitude on lean blow-off limits

Fig. 2 shows the lean blow out limits of the forced flames at 160 Hz, measured using the NPR and NPA configurations. The fuel velocity at

blow-off constitutes the average value of ten blow-off events, while the standard deviation of these measurements normalised by the mean value was approximately 0.03. It should be noted that this low value was made possible because the step of fuel flow rate reduction was very small (0.1 lpm) and a large number of blow-off measurements were conducted.

For both NPR and NPA flames, it can be deduced that forcing reduces the stability of the flame, which decreases with increasing forcing amplitude. In particular, for a constant $U_{air}$ at blow-off, the greater the forcing amplitude $A$, the greater the $U_f$ at blow-off, whereas for a constant $U_f$, the greater the forcing amplitude, the lower the $U_{air}$ at blow-off. Also, for a given forcing amplitude $A$, as the $U_f$ increases, the $U_{air}$ increases. This is consistent with the findings of previous studies on the blow-off behaviour of forced premixed flames [7,17] as well as with fundamental studies on laminar counterflow diffusion flames [4–6]. It was deduced that the acoustic forcing had a great influence on blow-off equivalence ratios, which was found to depend on the modulation frequency and mixture velocity. In addition, another study on blow-off of forced premixed flames with spatial mixture gradients [9] reported that the blow-off equivalence ratio increased with forcing amplitude for $f = 100$ Hz and $f = 200$ Hz. This was associated with the greater unsteadiness at the flame base, in agreement with the results of Balachandran et al. [15].

The NPA system shows a greater sensitivity to changes in forcing amplitude compared to the NPR configuration, since for a given air flow rate and forcing amplitude it exhibits larger variations of the fuel flow rate (overall equivalence ratio) compared to the case without forcing. For example, considering a constant $U_{air} = 15.7$ m/s, between $A = 0$ and $A = 0.25$, for the NPA system, $U_f$ changes in the range of 15.5–26.9 m/s (the maximum variation from the $U_f$ value at $A = 0$ is approximately 70%). In the NPR system, for $U_{air} = 15.7$ m/s, between $A = 0$ and $A = 0.25$, $U_f$ changes in the range of 15.0–16.1 m/s (the maximum variation from the $U_f$ value at $A = 0$ is approximately 7%). This implies that the operating range of the NPA system is significantly reduced in the presence of forcing. However, considering the global equivalence ratio at blow-off, it should be noted that the NPA system can be operated much leaner compared to the NPR system for all the forcing amplitudes investigated in this work. Therefore, the higher sensitivity of the NPA system to changes in the amplitude of the fluctuations could be attributed to the higher sensitivity typically associated to very lean conditions (small global equivalence ratio). The fluctuations of the air flow might have an important impact on the recirculation zone, changing significantly the mixing pattern and therefore affecting the lean blow out. In contrast, in the NPR system the higher equivalence ratio at blow-off (for a given air velocity at the inlet), also in the absence of forcing, indicates that this injection configuration is intrinsically less stable and this can be related to the injection location that causes the flame to be in a high strain region. The presence of air flow oscillations only slightly changes the operating range (already smaller compared to the NPA system). This also suggests that in the NPR case, the fluctuations of the air flow have a lower effect on the mixing pattern than that in the NPA case.

### 3.2. Blow-off event visualisation

As far as the unforced case NPR-15-050 is concerned (Fig. 3), the OH PLIF images demonstrate that the OH fluorescence signal is relatively continuous and concentrates mainly in a thin zone, located in the

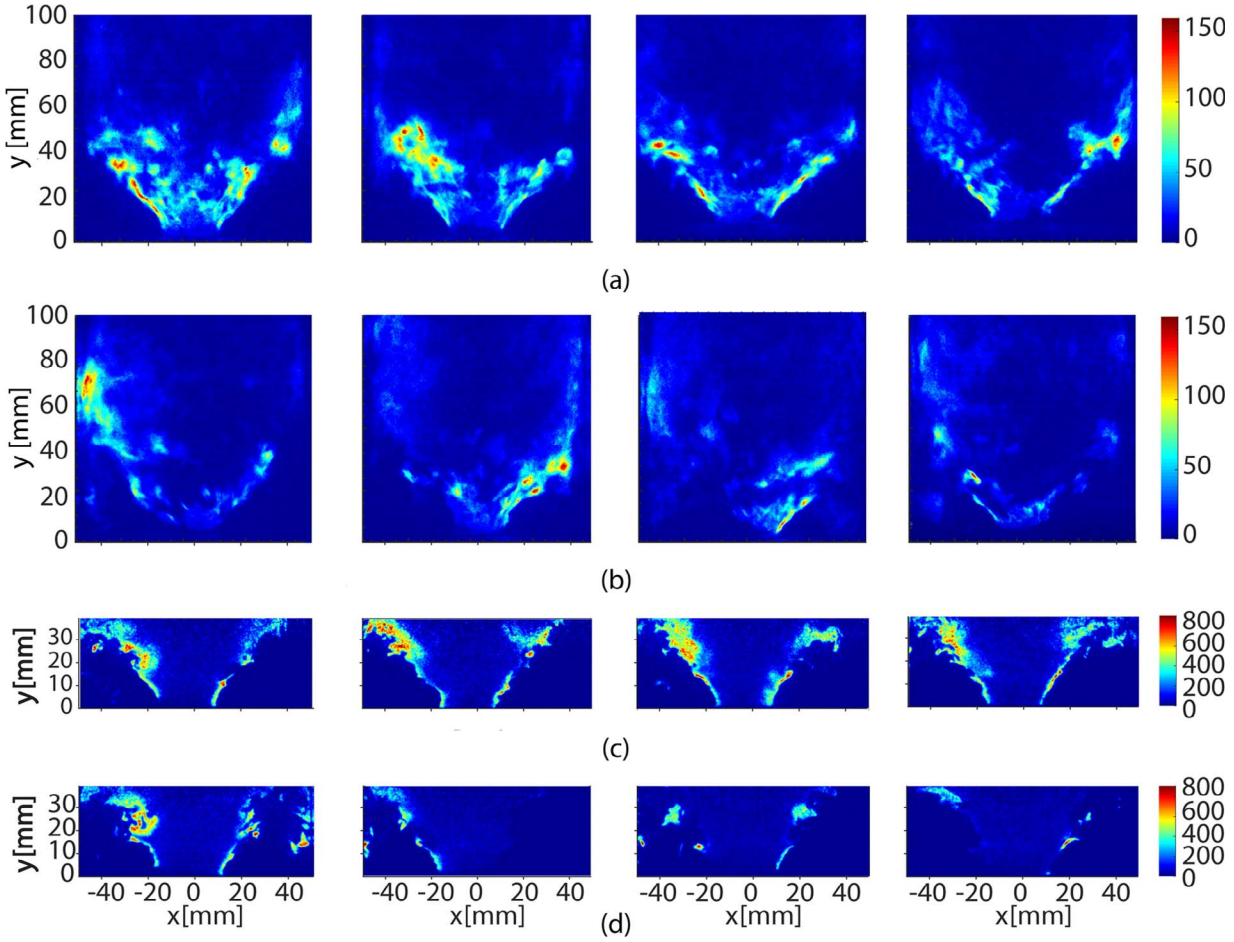


**Fig. 3.** Instantaneous OH* chemiluminescence images of (a) unforced stable flame NPR-15-050 and (b) forced blow-off flame NPR-15-050-160-15, and (c, d) the respective OH PLIF images. For the forced case, images correspond to 40, 20, 10 and 1 ms from blow-off.

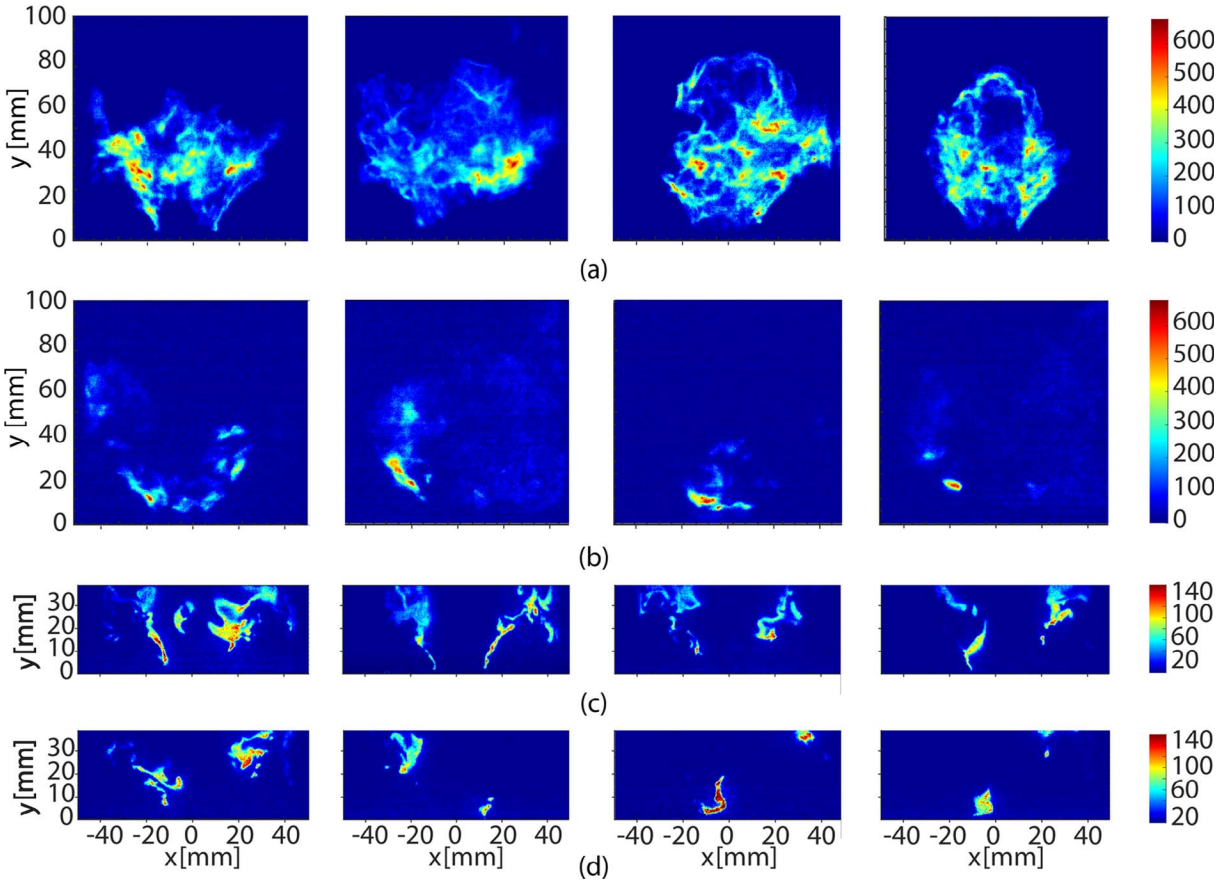


**Fig. 4.** Instantaneous OH* chemiluminescence images of (a) unforced stable flame NPA-15-030 and (b) forced blow-off flame NPA-15-030-160-15 and (c, d) the respective OH PLIF images. For the forced case, images correspond to 40, 20, 10 and 1 ms from blow-off.

inner shear layer (ISL) region, suggesting that the flame branches are anchored at the bluff body edge. For forced flame with radial injection, NPR-15-050-160-15, a decrease in the size of the heat release zone is observed, while the OH zone is fragmented in different regions. Complete or partial absence of the flame branch in the ISL and/or wall region, and attachment and lift-off at the bluff body edge can be seen. Concerning the unforced stable flame NPA-15-030 (Fig. 4), the OH PLIF images reveal that the OH fluorescence signal is relatively continuous, with occasional flame lift-off. The visualisation of the blow-off event for flame NPA-15-030-160-15 shows a gradual decrease in the size of the heat release zone, with the last flame fragments seen inside the inner recirculation zone and in the vicinity of the fuel nozzle exit. On the contrary, in the case of NPR-15-050-160-15, the last flame fragments during blow-off are observed in the ISL region. This is associated with the fact that in the NPA system the fuel is injected axially in the inner recirculation zone, whereas in the NPR system the fuel is injected radially upstream of the bluff body plane. As also observed in previous studies with swirling flames without forcing [12,13], as the flame approaches the blow-off, it becomes more and more fragmented with holes along the flame sheet, interpreted as local extinctions of the flame. The presence of local extinction and their evolution into a global blow-off has also been confirmed by advanced numerical simulations [18–20].

After the qualitative description of the blow-off event for both NPR and NPA flames, the duration of the blow-off transient, $t_B$, is quantified, as shown in Fig. 5. The beginning of the transient is defined as the last point in time at which the OH* chemiluminescence signal is at the steady-state mean value. Sufficiently far from blow-off, a nearly periodic response, with small variations in amplitude is observed, followed by a transition to zero OH* chemiluminescence signal as the complete extinction is approached. It is evident that the duration of the blow-off

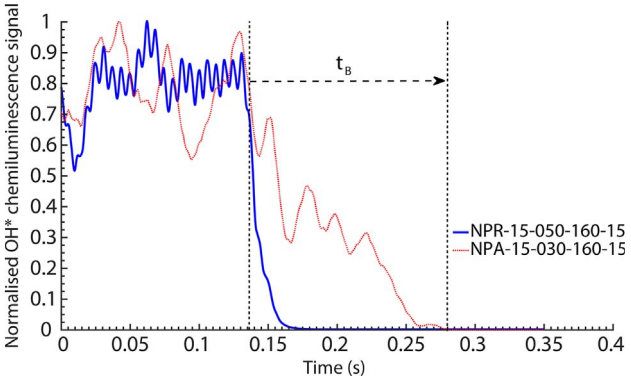


**Fig. 5.** Time series of OH* chemiluminescence signal, normalised by its maximum value, for flames NPR-15-050-160-15 and NPA-15-030-160-15, used to quantify the duration of the blow-off transient, $t_B$.

event is significantly greater for flame NPA-15-030-160-15 compared to the flame NPR-15-050-160-15 (147.2 ms vs 31.9 ms). Given that the two configurations have the same air bulk velocity, it could be suggested that this is attributed to the difference in the fuel injection configuration.

The blow-off event duration of flame NPA-15-030-160-15, which lasts for 23.5 cycles for the 160 Hz oscillation, is much greater than the average blow-off duration of unforced non-premixed flames (46.6 ms), measured in the same burner [12]. This is consistent with the results of a previous study on the response and extinction behaviour of laminar counterflow diffusion and premixed flames [4], which reported that the presence of oscillation retards extinction. In addition, it was found that the blow-off duration increases with forcing frequency and decreases

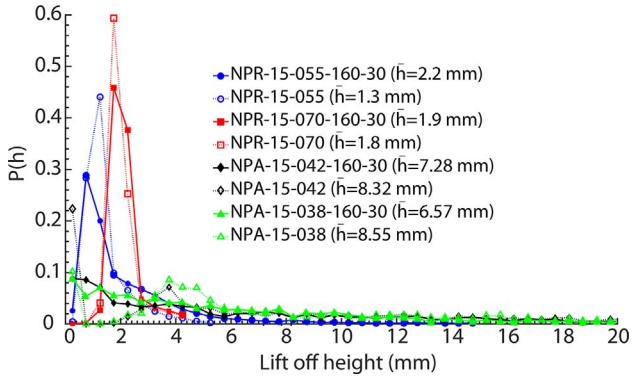


**Fig. 6.** Probability density function of the lift-off height, $P(h)$, for forced and unforced NPR and NPA flames. The average lift-off height, $\bar{h}$, is given in the legend.

with forcing amplitude.

The evaluation of the duration of the blow-off transient is very important for the development of control strategies to avoid the global extinction of the flame. The results obtained in this work show that the configuration with axial injection is characterised by a longer blow-off transient compared to the flame with radial injection. Furthermore, the great difference in the duration of the blow-off event in the two non-premixed systems investigated here suggests that the injection configuration and the degree of premixedness are crucial in determining the blow-off dynamics. As discussed in Ref. [20], the blow-off transient of non-premixed gaseous flames can be explained in terms of finite-chemistry effects that lead to local extinctions that eventually evolve in a global blow-off. The differences in the blow-off transient observed for the flames with axial and radial injection suggest that the two configurations may be characterised by different interactions between the flame and the mixing field. Therefore, these cases can be of great interest for the assessment and validation of the capability of numerical methods to capture the flame blow-off in a wide range of conditions.

### 3.3. Lift-off height analysis

In this section, the lift-off height statistics are investigated in stable flames, farther and closer to blow-off. Fig. 6 shows the probability density function (PDF) of the lift-off height, for both the forced and unforced NPR and NPA flames. The average lift-off height is also indicated in Fig. 6. For this calculation, the lift-off heights of the left and right branch of the flame in each instantaneous snapshot were considered as two independent samples.

For flames NPR-15-055-160-30 and NPR-15-055, the peaks of the PDFs reveal that 28% and 44% respectively of the samples exhibit a lift-off height of approximately 0.75 mm and 1.25 mm respectively, with the average lift-off height being 2.2 mm and 1.3 mm respectively. Farther from blow-off, flames NPR-15-070-160-30 and NPR-15-070 have a similar average lift-off height ($\bar{h}$ = 1.9 mm and $\bar{h}$ = 1.8 mm respectively), suggesting that forcing hardly affects the lift-off behaviour of the flame far from blow-off. The peaks reveal that 46% and 60% respectively of the samples exhibit a lift-off height approximately at 1.75 mm. In terms of time evolution of the lift-off height, the PSDs in Fig. 7 show that unlike the unforced case, the lift-off height of the forced flame shows periodicity at 160 Hz.

The lift-off heights of NPA flames are significantly more pronounced than those of NPR flames, while the PDFs of NPA system have a much longer positive tail than those of NPR system. Unlike NPR flames, the average lift-off height of forced NPA flames is lower than that of the respective unforced conditions. Close to blow-off, for stable flames NPA-15-038-160-30 and NPA-15-038, the peaks of the PDFs demonstrate that 0.09% and 0.1% of the samples respectively reveal a lift-off height below 0.25 mm. The average lift-off height is 6.57 mm and 8.55 mm for the forced and unforced flame respectively. Farther from

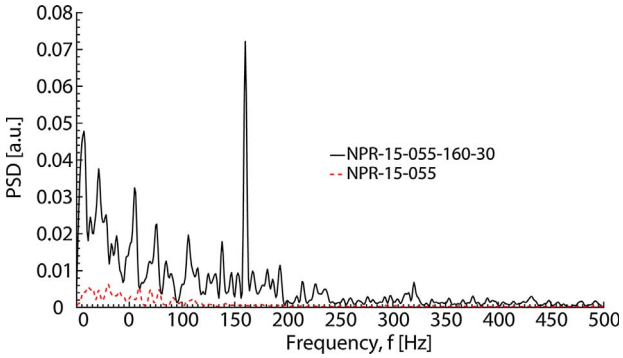


**Fig. 7.** Power spectral densities of the lift-off height for flames NPR-15-055 and NPR-15-055-160-30.

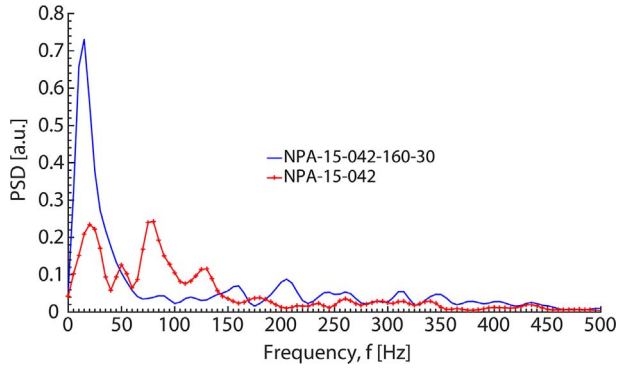


**Fig. 8.** Power spectral densities of the lift-off height for flames NPA-15-042 and NPA-15-042-160-30.

blow-off, the PDFs of flames NPA-15-042-160-30 and NPA-15-042 are similar, with the average lift-off height being 7.28 mm and 8.32 mm respectively. In the NPA flames, the lift-off height is not periodic at the forcing frequency, as concluded by the absence of the 160 Hz peak in the PSD (Fig. 8). The lower sensitivity to the forcing of the NPA system compared to the NPR system observed in the lift-off height is consistent with the heat release response analysed in a previous study [21], where it was shown that the NPR system exhibited a greater response to acoustic forcing compared to the NPA system. It should be noted that in the NPR system the location of the flame is closer to the strong acoustic oscillations at the exit of the annular air passage than that of the NPA system. However, as previously discussed, the NPA system seems to show a greater sensitivity to the forcing amplitude in terms of blow-off behaviour, which might be related to the very low global equivalence ratio that this configuration can reach without the presence of forcing.

The data shown here can help validate turbulent combustion models focusing on flame anchoring and stabilisation mechanisms. In particular, the fluctuations of the strain rate on the flame will need to be captured for an accurate prediction of local, and hence global extinction.

## 4. Conclusions

The effect of air fluctuations on the behaviour of nominally non-premixed swirling flames at conditions close to blow-off has been investigated using experiments with the main objective of extending forced flame studies towards the case of flames close to their overall stability limits. At the same time, typical lean blow out studies were extended to the case of forced air fluctuations. Two fuel injection geometries (radial and axial injection) were investigated that provide different mixture fraction patterns.

Results show that the fluctuations have a strong effect on the flame behaviour with a noticeable effect on the lean blow out limits. In both

configurations studied in this work, it was found that the acoustic forcing reduces the stability of the flame and the stability decreases with the increase in forcing amplitude. The system with axial injection showed a greater sensitivity to the forcing amplitude compared to the system with radial injection in terms of changes in the operability limits. Both systems, at the blow-off condition showed a gradual decrease in the flame size, with the flame sheet being fragmented in different regions, together with intermittent attachment and lift-off from the bluff-body. In both configurations investigated here, the last fragments of the flame were detected in the region close to the injection location suggesting that during the blow-off event the flame moves closer and closer to the fuel injection system. The duration of the blow-off event was found to be significantly greater in the case with axial injection, suggesting that the injection configuration and hence the mixture fraction pattern have an important effect on the blow-off dynamics.

The presence of forcing also affects the lift-off height. In particular, in the configuration with radial injection the spectrum of the lift-off height showed a clear peak at the forcing frequency. This peak is less evident in the spectrum of flames with axial injection suggesting again that the injection geometry and mixing behaviour may have an important impact on the dynamic response of the flame.

## Acknowledgements

The financial assistance of the EPSRC, Rolls-Royce Group, and Onassis Foundation is acknowledged.

## References

[1] S. Candel, D. Durox, T. Schuller, P. Palies, J.F. Bourgouin, J.P. Moeck, Progress and challenges in swirling flame dynamics, Comptes Rendus - Mecanique 340 (2012) 758–768.
[2] T. Poinsot, Prediction and control of combustion instabilities in real engines, Proc. Combust. Inst. 36 (2017) 1–28.
[3] A.P. Dowling, Y. Mahmoudi, Combustion noise, Proc. Combust. Inst. 35 (2015) 65–100.
[4] C.J. Sung, C.K. Law, Structural sensitivity, response, and extinction of diffusion and premixed flames in oscillating counterflow, Combust. Flame 123 (2000) 375–388.
[5] T.M. Brown, R.W. Pitz, C.J. Sung, Oscillatory stretch effects on the structure and extinction of counterflow diffusion flames, Symp. (Int.) Combust. 27 (1998) 703–710.
[6] J.S. Kistler, C.J. Sung, T.G. Kreut, C.K. Law, M. Nishioka, Extinction of counterflow diffusion flames under velocity oscillations, Symp. (Int.) Combust. 26 (1996) 113–120.
[7] A.A. Chaparro, B.M. Cetegen, Blowoff characteristics of bluff-body stabilized conical premixed flames under upstream velocity modulation, Combust. Flame 144 (2006) 318–335.
[8] S. Chaudhuri, S. Kostka, M.W. Renfro, B.M. Cetegen, Blowoff mechanism of harmonically forced bluff body stabilized turbulent premixed flames, Combust. Flame 159 (2012) 638–640.
[9] S. Chaudhuri, B.M. Cetegen, Blowoff characteristics of bluff-body stabilized conical premixed flames with upstream spatial mixture gradients and velocity oscillations, Combust. Flame 153 (2008) 616–633.
[10] S. Biswas, K. Kopp-Vaughn, M.W. Renfro, B.M. Cetegen, Phase resolved characterization of conical premixed flames near and far from blowoff, Combust. Flame 160 (2013) 2843–2855.
[11] S. Chaudhuri, B.M. Cetegen, Response dynamics of bluff-body stabilized conical premixed turbulent flames with spatial mixture gradients, Combust. Flame 156 (2009) 706–720.
[12] D.E. Cavaliere, J. Kariuki, E. Mastorakos, A comparison of the blow-off behaviour of swirl-stabilized premixed, non-premixed and spray flames, Flow Turbulence Combust 91 (2013) 347–372.
[13] R. Yuan, Measurements in Swirl-stabilised Spray Flames at Blow-off, Department of Engineering, University of Cambridge, Cambridge, 2015, p. 78.
[14] D.E. Cavaliere, Blow-off in gas turbine combustors, in: Department of Engineering, University of Cambridge, Cambridge, UK, 2013.
[15] R. Balachandran, B.O. Ayoola, C.F. Kaminski, A.P. Dowling, E. Mastorakos, Experimental investigation of the nonlinear response of turbulent premixed flames to imposed inlet velocity oscillations, Combust. Flame 143 (2005) 37–55.
[16] A.F. Seybert, D.F. Ross, Experimental determination of acoustic properties using a two-microphone random-excitation technique, J. Acoust. Soc. Am. 61 (1977) 1362–1370.
[17] A. Chaparro, E. Landry, B.M. Cetegen, Transfer function characteristics of bluff-body stabilized, conical V-shaped premixed turbulent propane–air flames, Combust. Flame 145 (2006) 290–299.
[18] A. Giusti, E. Mastorakos, Detailed chemistry LES/CMC simulation of a swirling ethanol spray flame approaching blow-off, Proc. Combust. Inst. 36 (2017) 2625–2632.
[19] H. Zhang, A. Garmory, D.E. Cavaliere, E. Mastorakos, Large Eddy simulation/conditional moment closure modeling of swirl-stabilized non-premixed flames with local extinction, Proc. Combust. Inst. 35 (2015) 1167–1174.
[20] H. Zhang, E. Mastorakos, Prediction of global extinction conditions and dynamics in swirling non-premixed flames using LES/CMC modelling, Flow Turbulence Combust 96 (2016) 863–889.
[21] A.M. Kypraiou, N.A. Worth, E. Mastorakos, Experimental investigation of the response of premixed and non-premixed turbulent flames to acoustic forcing, in: 54th AIAA Aerospace Sciences Meeting, American Institute of Aeronautics and Astronautics, 2016.